

Rev. 114, 201 (1959).

<sup>20</sup>P. R. Bevington, W. W. Roland, and H. W. Lewis, Phys. Rev. 121, 871 (1961).

<sup>21</sup>H. W. Lefevre and G. U. Din, Australian J. Phys. 22, 669 (1969).

<sup>22</sup>P. R. Borchers and C. H. Poppe, Phys. Rev. 129, 2679 (1963).

<sup>23</sup>J. B. Marion and T. W. Bonner, in *Fast Neutron Physics*, edited by J. B. Marion and J. L. Fowler (Interscience, New York, 1963), p. 1865.

<sup>24</sup>F. Gabbard, to be published.

<sup>25</sup>J. K. Dickens, private communication; J. K. Dickens, E. Eichler, I. R. Williams, and R. Kuebbing, Oak Ridge National Laboratory Report No. ORNL-4134, 1967 (un-

published), p. 22.

<sup>26</sup>M. S. Zisman and B. G. Harvey, Phys. Rev. C 5, 1031 (1972).

<sup>27</sup>The computer program used was ALTE modified to include the enhancement factor (Refs. 6 and 9). [W. R. Smith, Comput. Phys. Commun. 1, 106 and 181 (1970)]. Details are given in Refs. 1, 2, and 7.

<sup>28</sup>P. A. Moldauer, Phys. Rev. Letters 9, 17 (1962).

<sup>29</sup>K. H. Bhatt and J. B. Ball, Nucl. Phys. 63, 286 (1965).

<sup>30</sup>J. Vervier, Nucl. Phys. 75, 17 (1966).

<sup>31</sup>S. Chochavi and D. B. Fossan, Phys. Rev. C 3, 275 (1971).

<sup>32</sup>S. A. Hjorth, and B. L. Cohen, Phys. Rev. 135, B920 (1964).

## $\beta$ Decay of $^{168}\text{Ho}$ to Levels in $^{168}\text{Er}^\dagger$

K. G. Tirsell and L. G. Multhaus

Lawrence Livermore Laboratory, University of California, Livermore, California 94550

(Received 4 August 1972)

The  $\beta$  decay of  $^{168}\text{Ho}$  to levels in the strongly deformed  $^{168}\text{Er}$  nucleus has been studied using Ge(Li) spectroscopy. Over 150  $\gamma$  rays were observed, about half of which could be assigned to  $^{168}\text{Ho}$  decay. Among the rotational bands that have been identified in  $^{168}\text{Er}$  are the ground state, the  $\gamma$  band at 821.109 keV, and  $K^\pi=4^-$  and  $3^-$  bands at 1093.898 and 1541.33 keV, respectively. At higher energies, evidence was obtained for bands having energies ( $I^\pi K$ ) of 1848.20 ( $2^+2$ ), 1930.23 ( $2^+2$ ), 2192.97 ( $2^-2$ ), and 2424.87 ( $2^+2$ ) keV.  $\beta$ -decay  $\log ft$  values to levels of  $^{168}\text{Er}$  support a  $3^+3$  assignment for the  $^{168}\text{Ho}$  ground state.

### I. INTRODUCTION

The nucleus  $^{168}\text{Er}$  is doubly even and strongly deformed. Its energy-level properties have been studied in  $^{168}\text{Tm}$  decay,<sup>1-8</sup> thermal-neutron capture,<sup>9-11</sup> average-resonance neutron capture,<sup>12</sup> the ( $d, p$ ) reaction on  $^{167}\text{Er}$ ,<sup>13</sup> inelastic deuteron scattering,<sup>14</sup> and Coulomb excitation with  $^{16}\text{O}$  ions.<sup>15</sup> The properties of levels populated in  $^{168}\text{Tm}$  decay (up to 1715.71 keV) have been determined with the aid of  $\beta$  branching ratios, accurate  $\gamma$ -ray energies and intensities,  $\gamma$ - $\gamma$  coincidence and angular-correlation measurements, lifetime determinations, and conversion-electron spectra. Rotational bands that have been identified include the ground-state,  $\gamma$  vibration, and  $K^\pi=3^-$  and  $K^\pi=4^-$  bands with a two-quasineutron configuration.

Levels up to 2148 keV have been identified and are characterized by their population intensities in thermal- and average-resonance neutron capture (hereafter referred to as resonance-capture) studies. Levels were observed with spins from 0

to 8. Bands that were identified in addition to those seen in  $^{168}\text{Tm}$  decay include the  $\beta$  vibration and  $K^\pi=1^-$  and  $2^-$  octupole. Additional information on high-energy levels has been obtained from inelastic deuteron scattering, which populates strongly only collective levels. Both collective and two-quasineutron levels are populated in the ( $d, p$ ) reaction. Results of these studies are summarized in Fig. 1 and Table I.

The decay of  $^{168}\text{Ho}$  was first studied by Wille and Fink.<sup>16</sup> Takahashi *et al.*<sup>17</sup> measured a high-energy  $\beta$  group at 2.2 MeV and a  $\gamma$  peak at 850 keV. They determined the half-life to be  $3.3 \pm 0.5$  min. Haustein and Tucker<sup>18</sup> produced more intense  $^{168}\text{Ho}$  sources by irradiating  $^{170}\text{Er}$  with 70-MeV bremsstrahlung. Their spectra include primarily peaks for  $^{169}\text{Ho}$  and  $^{168}\text{Ho}$  produced by ( $\gamma, p$ ) and ( $\gamma, np$ ), respectively. They observed  $\gamma$  transitions from levels up to 994 keV. Since the  $Q$  value for  $^{168}\text{Ho}$  decay is 3.0 MeV,<sup>17</sup> it is reasonable to expect that levels in  $^{168}\text{Er}$  above 994 keV will be populated. Indeed, as this study has shown, levels with energies as high as or higher than

those observed in other studies are populated. Selection rules of  $\beta$  and  $\gamma$  decay contribute to the understanding of their properties.

## II. EXPERIMENTAL PROCEDURES

The  $^{168}\text{Ho}$  activity was produced by the  $^{168}\text{Er}(n, p)$  reaction on a 400-mg sample of Er oxide with an  $^{168}\text{Er}$  enrichment of 95.47%. The sample was bombarded with 14-MeV neutrons from the Livermore high-flux facility,<sup>19</sup> which produces greater than  $10^{12}$  neutrons per sec. The sample was irradiated for two half-lives, transported by a pneumatic rabbit system to the counting equipment, and counted for three half-lives. This cycle was repeated for several hours for each experimental configuration.

Measurements were made on three different

Ge(Li) detectors: a 6-cm<sup>3</sup> planar, a 25-cm<sup>3</sup> closed-end trapezoidal, and an 80-cm<sup>3</sup> closed-end coax, with resolution values of 2.3, 3.0, and 2.2 keV, respectively, for the 1333-keV line of  $^{60}\text{Co}$ . Conventional low-noise preamplifiers and amplifiers, a pileup rejector, and a Nuclear Data 4096-channel pulse-height analyzer were used. Zero and gain were stabilized with an ultrastable mercury-relay pulser.

Peak locations and areas were determined by the least-squares fitting of a modified Gaussian on a linear or quadratic background. The fitting code is further described in Ref. 20. Efficiency calibration of detectors was accomplished by using standard International Atomic Energy Agency (IAEA) sources, in addition to lines of well measured relative intensities in  $^{56}\text{Co}$ ,  $^{21}\text{Br}$ ,  $^{22,23}$  and  $^{180}\text{Hf}$ .<sup>24</sup> In general, errors in the relative-effi-

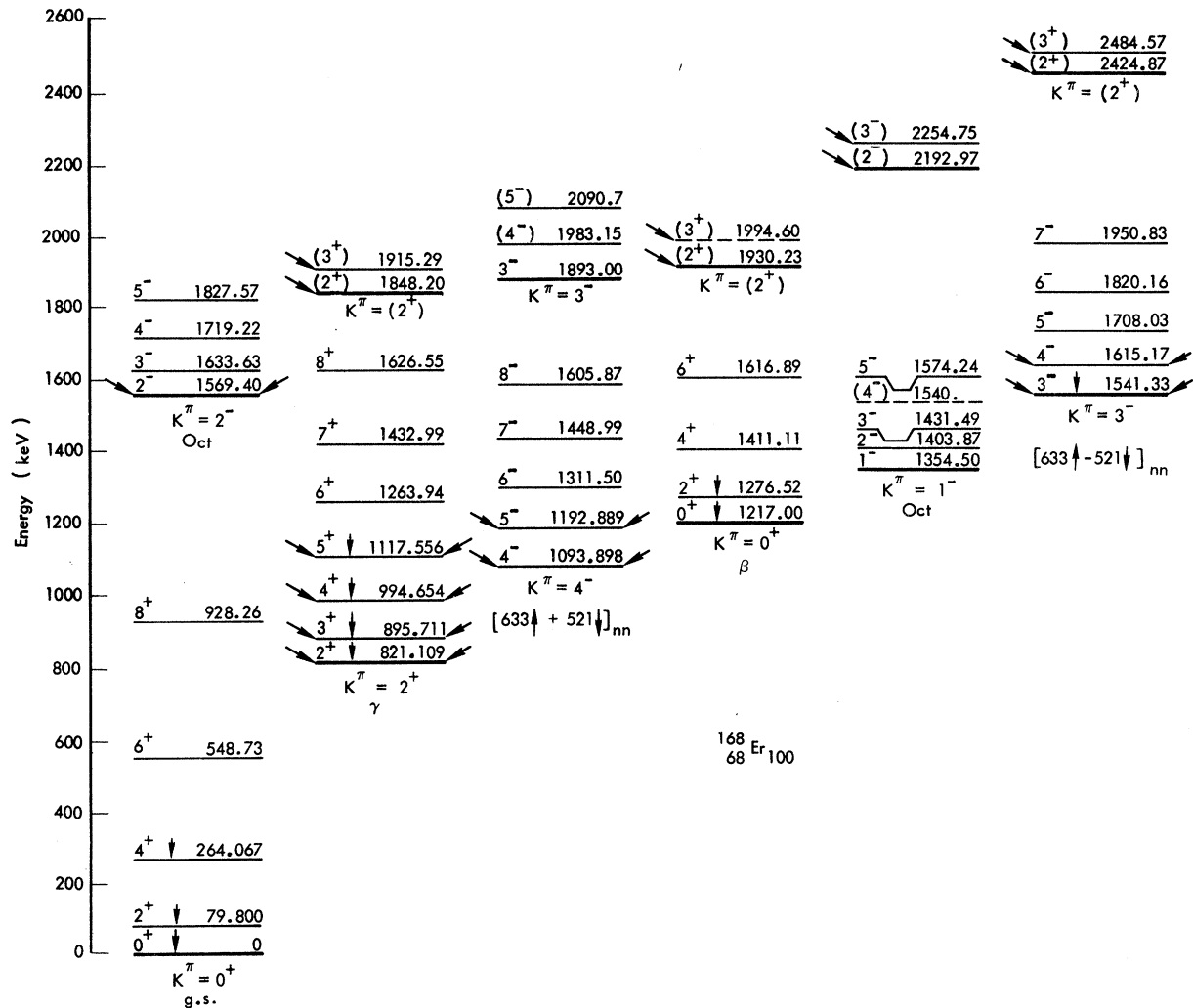


FIG. 1. Band structure of  $^{168}\text{Er}$ . Arrows denote the following decay modes:  $\searrow$ ,  $^{168}\text{Ho}$   $\beta$  decay;  $\downarrow$ ,  $\gamma$  transitions in  $^{168}\text{Ho}$  decay; and  $\swarrow$ ,  $^{168}\text{Tm}$   $\beta$  decay (Ref. 8). Other levels shown were identified in thermal-neutron capture (Ref. 11).

TABLE I. Levels identified in  $^{168}\text{Er}$ .

Present work	$(n, \gamma)^a$	Average-resonance $n$ capture <sup>b</sup>		$(d, d')^c$	$(d, p)^d$	$^{168}\text{Tm}^e$				
79.8	2 <sup>+</sup> 0	79.800	2 <sup>+</sup> 0	79.5	2, 5 <sup>+</sup>	80	79	2 <sup>+</sup> 0	79.82	2 <sup>+</sup> 0
264.067	4 <sup>+</sup> 0	264.081	4 <sup>+</sup> 0	263.6	3, 4 <sup>+</sup>	263	264	4 <sup>+</sup> 0	264.11	4 <sup>+</sup> 0
(548.45)		548.727	6 <sup>+</sup> 0	548.0		550	550	6 <sup>+</sup> 0	548.22	6 <sup>+</sup> 0
821.109	2 <sup>+</sup> 2	821.21	2 <sup>+</sup> 2	821.1	2, 3 <sup>+</sup>	821	823	2 <sup>+</sup> 2	821.12	2 <sup>+</sup> 2
895.711	3 <sup>+</sup> 2	895.84	3 <sup>+</sup> 2	895.9	3, 4 <sup>+</sup>		899	3 <sup>+</sup> 2	895.77	3 <sup>+</sup> 2
		928.26	8 <sup>+</sup> 0			926	~933	8 <sup>+</sup> 0		
994.654	4 <sup>+</sup> 2	994.79	4 <sup>+</sup> 2	994.2	3, 4 <sup>+</sup>	994	998	4 <sup>+</sup> 2	994.72	4 <sup>+</sup> 2
1093.898	4 <sup>-</sup> 4	1094.08	4 <sup>-</sup> 4	1094.0	3, 4 <sup>-</sup>		1094	4 <sup>-</sup> 4	1094.01	4 <sup>-</sup> 4
1117.56	5 <sup>+</sup> 2	1117.62	5 <sup>+</sup> 2	1116.9	2, 5 <sup>+</sup>		~1110	5 <sup>+</sup> 2	1117.58	5 <sup>+</sup> 2
1192.89	5 <sup>-</sup> 4	1193.06	5 <sup>-</sup> 4	1193.2	2, 5 <sup>-</sup>	1189	1193	5 <sup>-</sup> 4	1193.07	5 <sup>-</sup> 4
		1217.0	0 <sup>+</sup> 0							
		1263.94	6 <sup>+</sup> 2			1261	~1265	6 <sup>+</sup> 2		
		1276.52	2 <sup>+</sup> 0	1276.5	2, 5 <sup>+</sup>					
		1311.50	6 <sup>-</sup> 4				1312	6 <sup>-</sup> 4		
		1354.50	1 <sup>-</sup> 1			1357	1357			
		1403.87	2 <sup>-</sup> 1	1403.9	2, 5 <sup>-</sup>		1397			
		1411.11	4 <sup>+</sup> 0	1411.3	+					
		1431.49	3 <sup>-</sup> 1	1431.4	-	1428	3 <sup>-</sup>	1427	1431.41	3 <sup>-</sup>
		1432.99	7 <sup>+</sup> 2							
		1448.99	7 <sup>-</sup> 4			1445	1452	7 <sup>-</sup> 4		
		1493.45	3, 4 <sup>+</sup>	1493.2	3, 4 <sup>+</sup>					
1541.33	3 <sup>-</sup> 3	1541.60	(3-3)	1541.9	3, 4 <sup>-</sup>	~1538	1542	3 <sup>-</sup> 3	1541.48	3 <sup>-</sup> 3
		1541.60	(4 <sup>-</sup> 1)	1541.9						
1569.40	2 <sup>-</sup> 2	1569.46	2 <sup>-</sup> 2	1569.7	2, 5 <sup>-</sup>				1569.44	2, 3 <sup>-</sup>
		1574.24		1573.9	2, 5 <sup>-</sup>					
		1605.87	8 <sup>-</sup>				~1605	8 <sup>-</sup> 4		
1615.17	4 <sup>-</sup> 3	1615.38	4 <sup>-</sup>	1615.3	3, 4 <sup>-</sup>		~1615	4 <sup>-</sup> 3	1615.30	4 <sup>-</sup> 3
		1616.89	6 <sup>+</sup>							
		1626.55	8 <sup>+</sup>							
		1633.63	3 <sup>-</sup>	1633.4	3, 4 <sup>-</sup>	1630	(3 <sup>-</sup> )			
		1653.68	(4 <sup>+</sup> )	1652.0	3, 4 <sup>+</sup>					
		1656.53	(3 <sup>+</sup> )4 <sup>+</sup>	1655.8	3, 4 <sup>+</sup>					
		1693								
		1708.03	5 <sup>-</sup> 3	1708.3	2, 5 <sup>-</sup>		1709	5 <sup>-</sup> 3		
		1715.71	4, 5 <sup>+</sup>							
		1719.22	4 <sup>-</sup> 2							
		1728								
		1737.55	4 <sup>+</sup>	1736.5	3, 4 <sup>+</sup>	1733	(3 <sup>-</sup> , 4 <sup>+</sup> )			
		1820.16	6 <sup>-</sup> 3							
		1820.31	3, 4 <sup>-</sup>	1820.6	3, 4 <sup>-</sup>					
		1827.57	5 <sup>-</sup> 2	1828.3	2, 5 <sup>-</sup>		1826	6 <sup>-</sup> 3		
		1828.3	3, 4 <sup>-</sup>							
		1837								
1848.20	(2 <sup>+</sup> 2)	(1848)		1848.3	2, 5 <sup>+</sup>	1843				
		1886								
		1893.00	3 <sup>-</sup> 3	1893.7	3, 4 <sup>-</sup>		1897			
		1902								
		1905		1906.3	3, 4 <sup>-</sup>					
		1914.36	3 <sup>-</sup> (0)	1914.0	3, 4 <sup>-</sup>	1910	(3 <sup>-</sup> , 4 <sup>+</sup> )			
1915.29	(3 <sup>+</sup> 2)									
1930.23	(2 <sup>+</sup> 2)			1930.8	+					
		1950.83	7 <sup>-</sup> 3				(~1944)	7 <sup>-</sup> 3		
		1972.4	2, 5 <sup>-</sup>							
		1983.15	(4 <sup>-</sup> 3)	1983.1	2, 5 <sup>-</sup>					
(1994.60)	(3 <sup>+</sup> 2)	1998		1995.6	2, 5 <sup>-</sup>					
				2000.1	3, 4 <sup>-</sup>					
				2022.2	3, 4 <sup>-</sup>					

TABLE I (Continued)

Present work	$(n, \gamma)^a$	Average-resonance $n$ capture <sup>b</sup>	$(d, d')^c$	$(d, p)^d$	$^{168}\text{Tm}^e$
		2031.4 +			
		2056.0		2052	
		2060.1 3, 4 <sup>-</sup>			
		2080.9			
	2090.4 (5 <sup>-</sup> 3)			(2089)	
				(2102)	
		2108.9 +			
		2129.2 2, 5 <sup>-</sup>			
				2136	
		2148.40 2, 5 <sup>-</sup>			
			2170		
2192.97 (2 <sup>-</sup> 2)					
				2228	
2254.75 (3 <sup>-</sup> 2)			2257 3 <sup>-</sup>	2255	
			2274		
				2309	
				2335	
2424.87 (2 <sup>+</sup> 2)				2430	
				2446	
2484.57 (3 <sup>+</sup> 2)				(2478)	

<sup>a</sup> See References 10 and 11.<sup>b</sup> See Reference 12.<sup>c</sup> See Reference 14.<sup>d</sup> See Reference 13.<sup>e</sup> See Reference 8.

ciency curves were 5% below 200 keV, 3% from 200 to 3500 keV, and 5% above 3500 keV. In practice, however, the errors used were computed from error matrices derived from least-squares fits to the calibration data. Separate fits were made in the low-energy (to about 500 keV), middle-energy (about 300 to 2500 keV), and high-energy (above about 1800 keV) regions. The three fits were then joined to produce a single efficiency-vs-energy curve. Errors were smallest over the range of energies covered by  $^{56}\text{Co}$  lines. Total  $\gamma$ -ray intensity errors are the sum in quadrature of the  $\gamma$ -ray fitting error, the peak-efficiency error, an error due to effects of variations in the source-to-detector distance, and errors in summing corrections. The peak-efficiency contribution to errors in intensity ratios is a function of the energy difference between the pair of  $\gamma$  rays involved; as the energy difference approaches zero, the peak-efficiency error also approaches zero.

Relative half-lives were determined by comparing spectra taken at different times with respect to the end of irradiation. Each spectrum was a sum of data from a number of runs. By comparing peak areas and assigning the correct  $^{168}\text{Ho}$  half-life to a strong known peak, half-life values and errors could be determined for other peaks in the spectra.

Energy calibration of prominent  $^{168}\text{Ho}$  lines was accomplished by simultaneously accumulating data on calibration sources and the  $^{168}\text{Ho}$  sample. The

prominent lines were then used as an internal calibration to determine energies of the weaker lines. The nonlinearity of the electronic system was measured by using a large number of standard  $\gamma$ -ray lines accumulated in a single spectrum. A polynomial was least-squares fitted to the peak-centroid locations and  $\gamma$ -ray energies. The procedure is described more fully in Ref. 20.

### III. EXPERIMENTAL RESULTS

Figure 2 shows the  $\gamma$ -ray spectrum from 0 to 1.3 MeV taken with the 80-cm<sup>3</sup> diode. A low conversion gain of 0.34 keV/channel was used to allow good definition of multiplet peak shapes. A high-energy spectrum (1 to 4 MeV), also obtained using the 80-cm<sup>3</sup> diode, is shown in Fig. 3. The corresponding energy calibrations are shown in Tables II, III, and IV. Peak centroids of energy standards listed in Table II were least-squares fitted with fifth-order polynomials to determine the system nonlinearities for the low- and high-energy spectra. Values of  $\Delta E$  refer to the difference between the standard and fitted energies ( $E_{\text{std}} - E_{\text{fit}}$ ).

The  $^{168}\text{Ho}$   $\gamma$  rays listed in Table III were used to internally calibrate the low-energy spectrum. The  $^{168}\text{Ho}$  lines were measured by simultaneously accumulating data on both the source and the standards indicated in the table. For the high-energy spectrum,  $\gamma$  rays used as internal standards in-

cluded lines from  $^{168}\text{Ho}$  measured in the low-energy spectrum, and  $^{28}\text{Al}$  and  $^{24}\text{Na}$  lines, which appear in the source due to activation of silicon and aluminum contaminants. Two other contaminant lines ( $^{56}\text{Mn}$  with an energy<sup>25</sup> of  $1810.712 \pm 0.036$  keV and  $^2\text{H}$  at  $2223.29 \pm 0.07$  keV<sup>26</sup>) appear as singlets and are in agreement to within error with the calibration used, but were not included in the calibration.

A list of observed  $\gamma$  rays is given in Table V. Included are intensity values and placements in the  $^{168}\text{Ho}$  decay scheme. Most  $\gamma$  rays with half-lives too long or too short to be identified with the  $^{168}\text{Ho}$  3.3-min decay are not included.

#### IV. LEVEL SCHEME FOR $^{168}\text{Er}$ AND DISCUSSION

Our proposed  $^{168}\text{Er}$  level scheme is shown in Figs. 1 and 4. Placements of  $\gamma$  rays are based

primarily on the consistency of  $\gamma$  cascades using our accurate  $\gamma$ -ray energy values. Use has also been made of previous work.<sup>8,11-13</sup> Relative  $\beta$ -decay intensities were determined from the required intensity balance for the population and decay of levels.  $\log ft$  values were based on the assumption of no  $\beta$  feeding of the ground state, as supported by the  $\beta$ -spectrum measurement of Takahashi.<sup>17</sup>  $\beta$  decay to the ground state of  $^{168}\text{Er}$  from the  $3^+$  ground state of  $^{168}\text{Ho}$  (see Sec. IV B) is highly forbidden. A summary is presented in Table VI of  $I^\pi K$  assignments,  $\beta$  population intensities, and  $\log ft$  values for levels populated in  $^{168}\text{Ho}$  decay.

#### A. Ground-State Band

Levels of the ground-state rotational band at 79.800 and 264.067 keV are fed from several higher-lying levels. The intensity balance of  $\gamma$  transi-

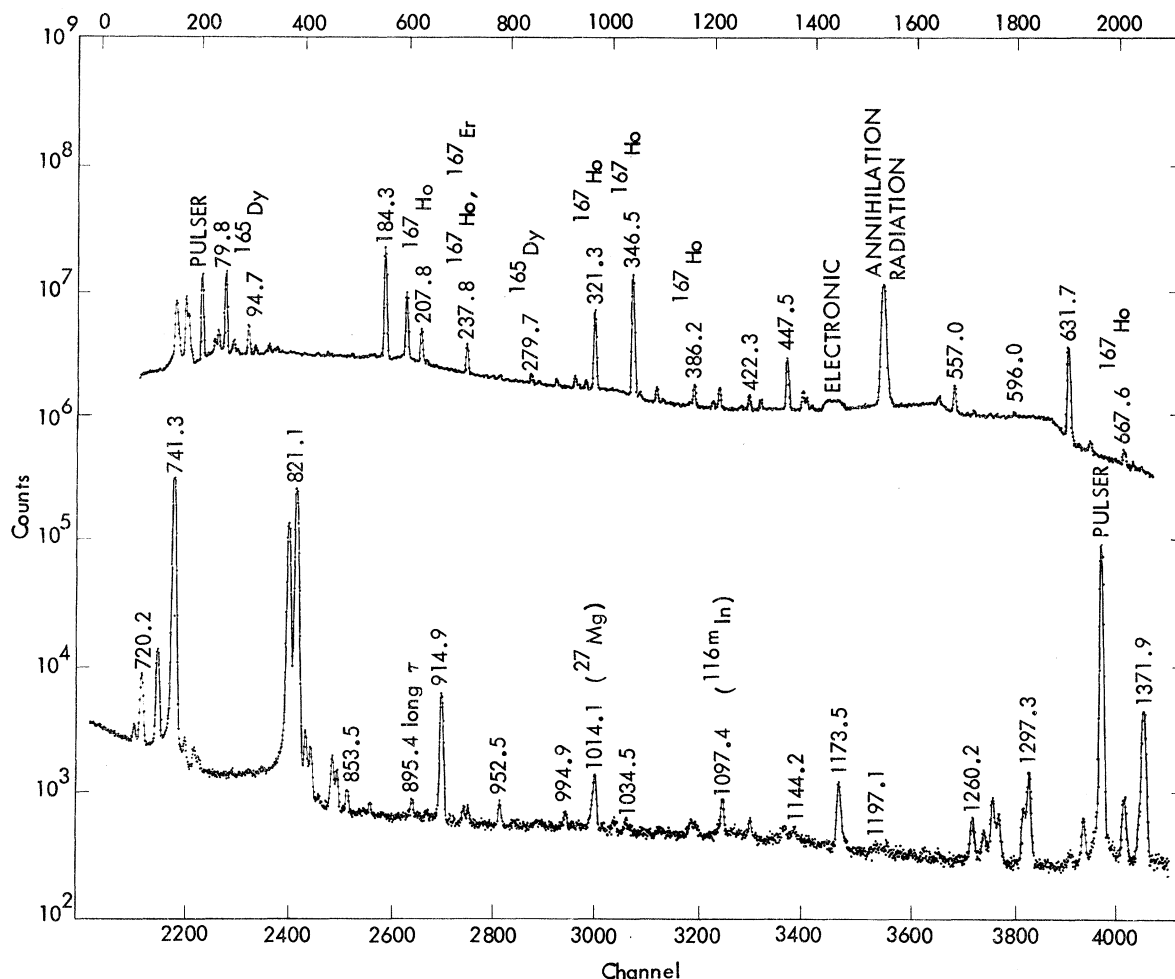


FIG. 2.  $\gamma$ -ray spectrum of  $^{168}\text{Ho}$  from 0 to 1.3 MeV. Counts in region labeled "electronic" are due to the absence of an upper-level discriminator on the analyzer when the data were taken.

tions indicates that there is no  $\beta$  feeding of either level. The  $284.47 \pm 0.07$ -keV  $\gamma$  ray may be the  $6^+ - 4^+$  transition observed in other studies.<sup>8, 10, 11</sup> However, an inconsistency in reported energies (Koch<sup>10</sup> reports a value of  $284.646 \pm 0.010$ , whereas Keller, Zganjar, and Pinajian<sup>8</sup> measured a value of  $284.11 \pm 0.11$  keV) and the lack of other evidence for population of the  $6^+$  level leaves the assignment uncertain.

Levels of the ground-state band have been observed up to spin 8. Properties of the band have been described by previous investigators.<sup>5</sup> The depression of energy levels is indicated by the coefficients given by Koch<sup>10</sup> for the third-order  $I(I+1)$  energy-sequence equation, which are:

$$A = 13.3428 \text{ keV} \pm 0.4 \text{ eV},$$

$$B = -7.23 \pm 0.03 \text{ eV},$$

$$C = 14.6 \pm 1 \text{ meV}.$$

#### B. $\gamma$ -Vibrational Band and Ground State of $^{168}\text{Ho}$

Levels of the  $\gamma$ -vibrational band with spins from 2 to 8 have been identified in  $(n, \gamma)$  studies.<sup>10, 11</sup> In our work we have observed the  $2^+$ ,  $3^+$ ,  $4^+$ , and  $5^+$  levels at 821.109, 895.711, 944.654, and 1117.56 keV, respectively.

$\gamma$  branching ratios, listed in Table VII, are in good agreement with results of other investigators<sup>5, 7, 8, 10, 11</sup> and are consistent with an average band-mixing parameter ( $z_2$ ) of  $0.0367 \pm 0.0021$  (compared, for example, to a value of  $0.0388 \pm 0.0015$  obtained by Gunther and Parsignault<sup>5</sup>). Mixing of the  $\gamma$ -vibrational and ground-state bands has been studied intensively by Gunther and Parsignault using several theoretical models, both macroscopic and microscopic. They conclude that existing calculations indicate a weaker mixing of the  $\gamma$ -vibrational and ground-state bands than ob-

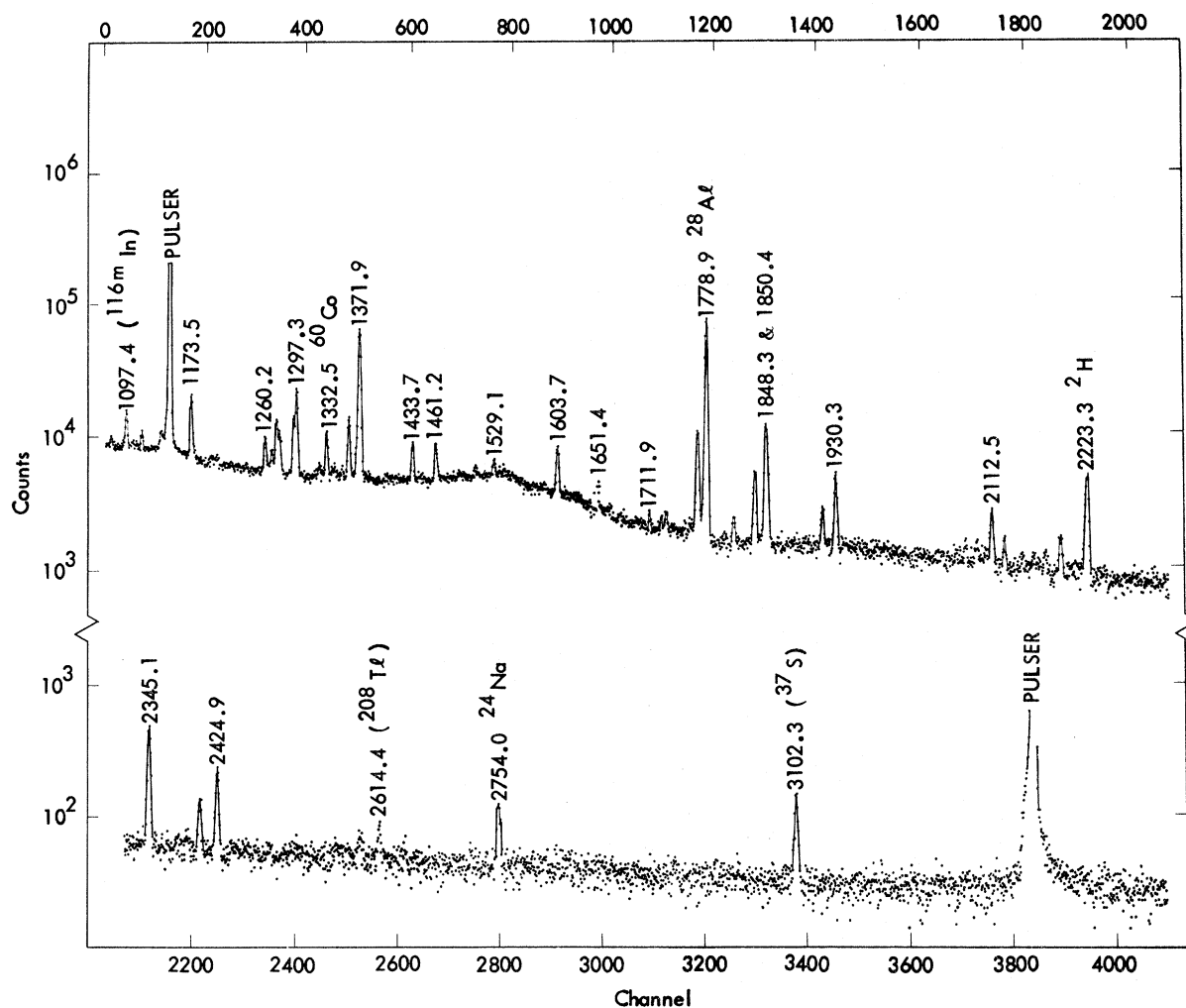


FIG. 3.  $\gamma$ -ray spectrum of  $^{168}\text{Ho}$  from 1 to 4 MeV.

TABLE II.  $\gamma$  rays used to measure spectrometer nonlinearities.

Source	Energy	Reference	$\Delta E$ of fit low-energy spectrum <sup>a</sup>	$\Delta E$ of fit high-energy spectrum <sup>a</sup>
<sup>57</sup> Co	122.063 ± 0.004	25	0.000	
<sup>139</sup> Ce	165.853 ± 0.007	b	0.000	
<sup>203</sup> Hg	279.188 ± 0.006	b	-0.001	
<sup>51</sup> Cr	320.078 ± 0.008	b	0.002	
<sup>198</sup> Au	411.794 ± 0.008	25	-0.002	
<sup>207</sup> Bi	569.689 ± 0.013	25	0.004	
<sup>137</sup> Cs	661.638 ± 0.019	25	-0.006	
<sup>54</sup> Mn	834.827 ± 0.021	25	0.003	
<sup>88</sup> Y	898.021 ± 0.019	25	-0.002	
<sup>207</sup> Bi	1063.635 ± 0.024	25	0.001	
<sup>65</sup> Zn	1115.518 ± 0.025	25	0.001	0.000
<sup>60</sup> Co	1173.208 ± 0.025	25	-0.001	0.002
<sup>22</sup> Na	1274.511 ± 0.028	25	0.000	-0.009
<sup>60</sup> Co	1332.483 ± 0.046	c		0.007
<sup>124</sup> Sb	1690.94 ± 0.04	24		0.000
<sup>207</sup> Bi	1770.17 ± 0.04	24		0.004
<sup>88</sup> Y	1836.02 ± 0.04	24		-0.002
<sup>124</sup> Sb	2090.92 ± 0.04	24		-0.003
<sup>208</sup> Tl	2614.48 ± 0.09	24		0.000
<sup>24</sup> Na	2753.98 ± 0.09	24		0.001

<sup>a</sup> Difference between measured energy and polynomial fit of measured values.

<sup>b</sup> R. C. Greenwood, R. G. Helmer, and R. J. Gehrke, Nucl. Instr. Methods **77**, 141 (1970).

<sup>c</sup> G. Murray, R. L. Graham, and J. S. Geiger, Nucl. Phys. **63**, 353 (1965).

served experimentally.

The structure of the  $\gamma$  band has been studied by Bès *et al.*<sup>27</sup> According to their calculations, four configurations have sizable amplitudes in the  $\gamma$  band; these are the two-neutron configurations [521 $\uparrow$  + 521 $\downarrow$ ] and [523 $\downarrow$  - 521 $\downarrow$ ] and the two-proton configurations [411 $\uparrow$  + 411 $\uparrow$ ] and [411 $\downarrow$  - 413 $\downarrow$ ].

The  $\beta$  decay of <sup>168</sup>Ho proceeds strongly to the 2<sup>+</sup>, 3<sup>+</sup>, and 4<sup>+</sup> members of the  $\gamma$  band. This, along with the absence of  $\beta$  decay to the ground state,

strongly suggests an  $I^\pi K$  assignment of 3<sup>+</sup>3.

Logft values to the first four levels of the  $\gamma$  band are 5.6, 6.2, 7.1, and 8.7. The first three values compare well with theory<sup>28</sup> for allowed decays, which gives ratios of 5.7/6.2/7.0. The logft for  $\beta$  population of the 5<sup>+</sup> level is expected to be large ( $\geq 10$ ), which is inconsistent with the value of 8.7 we have obtained. However, the presence of a small detectable amount of  $\gamma$  feeding of the 5<sup>+</sup> level could greatly alter the logft value.

TABLE III. Calibration of low-energy internal standards.

Source	Energy	$\Delta E$ of fit calibration spectrum <sup>a</sup>	$\Delta E$ of fit low-energy spectrum <sup>a</sup>
<sup>139</sup> Ce	165.853 ± 0.007	0.000	
Ho line	184.276 ± 0.020		0.001
Ho line	198.230 ± 0.020		0.009
Ho line	346.505 ± 0.020		-0.004
Ho line	447.450 ± 0.024		-0.011
<sup>137</sup> Cs	661.638 ± 0.019	0.001	
Ho line	741.293 ± 0.028		-0.005
Ho line	815.910 ± 0.029		0.007
Ho line	821.096 ± 0.029		0.003
<sup>54</sup> Mn	834.840 ± 0.021	-0.001	

<sup>a</sup> Difference between measured energy and polynomial fit of measured values.

TABLE IV. High-energy lines used as internal standards.

Source	Energy	Reference	$\Delta E$ of fit
Ho line	$1297,300 \pm 0.050$		-0.002
Ho line	$1358,996 \pm 0.050$		0.004
$^{27}\text{Al}$ contaminant	$1778,940 \pm 0.050$	25	0.000
$^{24}\text{Na}$ contaminant	$2753.98 \pm 0.09$	25	0.001

The most probable  $pn$  configuration of the ground state of  $^{168}\text{Ho}$ , based on level systematics in the region, is  $[523\uparrow - 521\uparrow]$ . This configuration can couple with the  $[523\uparrow - 521\uparrow]$  component of the  $\gamma$  band by an allowed unhindered  $\beta$  transition requiring a change of one quasiparticle. The low measured  $\log ft$  value is in good agreement with this supposition.

C.  $K\pi = 4^-$  Band at 1093.898 keV

Levels of the 1093.898-keV band have been observed in  $(n, \gamma)^{10,11}$  and  $(d, p)^{13}$  studies up through the  $8^-$  level at 1605.85 keV. The ground state of  $^{168}\text{Ho}$  populates the  $4^-$  and  $5^-$  levels at 1093.898 and 1192.89 keV, respectively. Table VIII shows the  $\gamma$  rays that deexcite these levels as measured

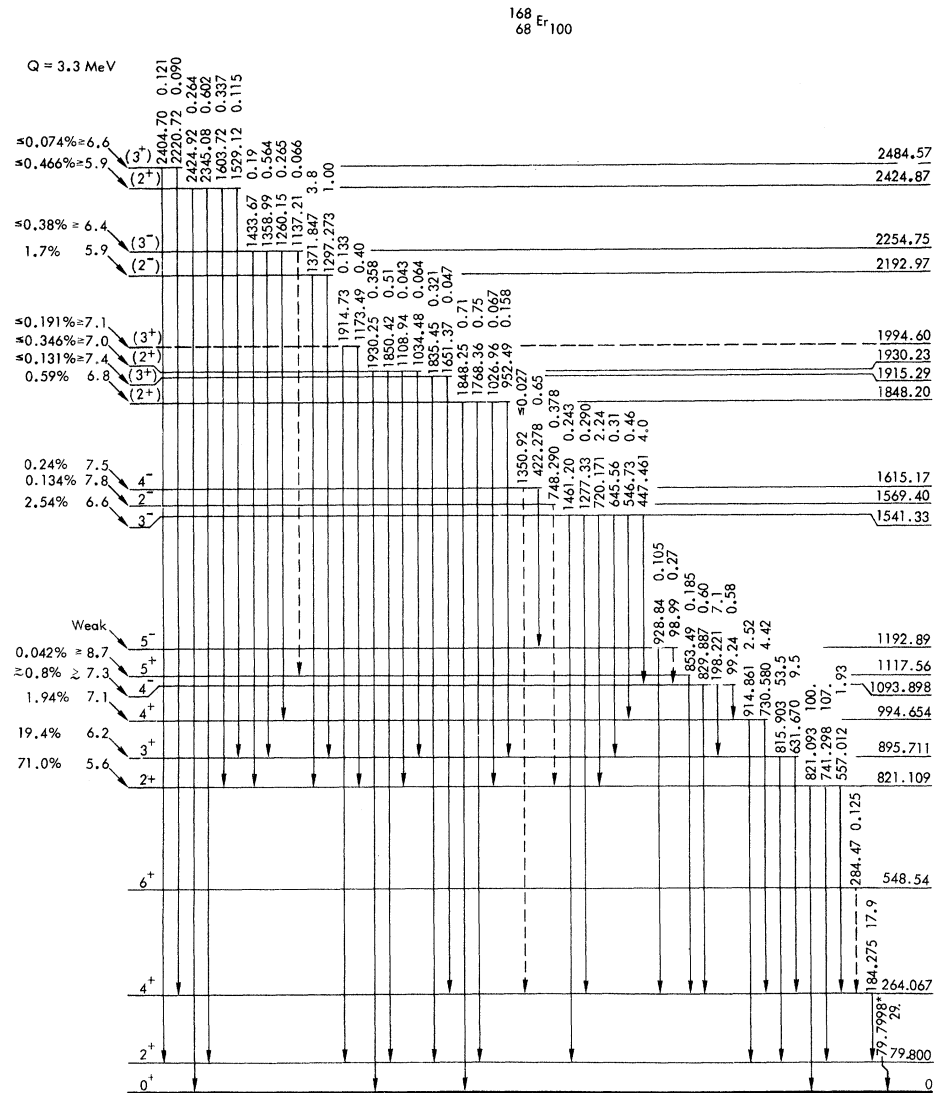


FIG. 4. Decay scheme of  $^{168}\text{Ho}$ . The asterisk denotes energies taken from Koch (Ref. 10).



TABLE V.  $\gamma$  rays observed in  $^{168}\text{Ho}$  decay spectra. <sup>a</sup>

Present work		Assignment From-To	$(n, \gamma)^b$	$^{168}\text{Tm}^c$	$^{168}\text{Ho}^d$
$E_\gamma$ (keV)	$I_{\text{rel}}$		$E_\gamma$ (keV)	$E_\gamma$ (keV)	$E_\gamma$ (keV)
79.833 ± 0.030	29 ± 6	80 → 0	79.7998 ± 0.0011	79.82 ± 0.02 99.05 ± 0.08	79.82 <sup>e</sup>
99.215 ± 0.030	0.85 ± 0.15	1094 → 995	99.285 ± 0.015	99.29 ± 0.02	
146.40 ± 0.06	0.113 ± 0.013	( <sup>34m</sup> Cl)			
162.44 ± 0.08	0.11 ± 0.03				
171.10 ± 0.13	0.042 ± 0.008	( <sup>27</sup> Mg)			
173.83 ± 0.09	0.062 ± 0.009	long $\tau$		173.8 ± 0.3	
184.275 ± 0.020	17.9 ± 2.0	264 → 80	184.281 ± 0.003	184.30 ± 0.02	184.30 <sup>e</sup>
198.221 ± 0.020	7.1 ± 1.5	1094 → 896	198.236 ± 0.003	198.25 ± 0.02	
209.20 ± 0.19	0.09 ± 0.03				
217.44 ± 0.10	0.062 ± 0.016		217.420 ± 0.006 272.87 ± 0.05	272.87 ± 0.09	
284.47 ± 0.07	0.125 ± 0.020	(549 → 264)	284.646 ± 0.010	284.11 ± 0.11	
297.77 ± 0.25	0.040 ± 0.014		(297.44 ± 0.25)		
365.71 ± 0.07	0.121 ± 0.014		365.64 ± 0.03		
381.67 ± 0.19	0.057 ± 0.012		381.38 ± 0.08		
383.62 ± 0.08	0.148 ± 0.012		(383.50 ± 0.25)		
422.278 ± 0.029	0.65 ± 0.06	1615 → 1193	422.302 ± 0.025	422.24 ± 0.11	
429.786 ± 0.036	0.386 ± 0.018		429.70 ± 0.04		
447.461 ± 0.024	4.0 ± 0.3	1541 → 1094	447.519 ± 0.025	447.47 ± 0.02	
457.592 ± 0.027	0.88 ± 0.03		457.64 ± 0.04		
546.73 ± 0.06	0.46 ± 0.05	1541 → 995		546.76 ± 0.03	
557.012 ± 0.027	1.93 ± 0.12	821 → 264	(557.00 ± 0.25)	557.08 ± 0.14	557.2
559.17 ± 0.26	0.066 ± 0.024				
569.50 ± 0.06	0.231 ± 0.017				
579.92 ± 0.10	0.148 ± 0.017				579.6 ± 0.5
596.02 ± 0.09	0.183 ± 0.019				
631.670 ± 0.027	9.5 ± 0.5	896 → 264	631.75 ± 0.04	631.66 ± 0.02	609.6 ± 0.5
645.56 ± 0.04	0.31 ± 0.04	1541 → 821		645.71 ± 0.03	631.9 ± 0.5
					656.4 ± 0.5
					663.4 ± 0.5
673.48 ± 0.13	0.106 ± 0.014	long $\tau$	673.50 ± 0.10	673.68 ± 0.09	
679.08 ± 0.15	0.088 ± 0.014				
720.171 ± 0.030	2.24 ± 0.11	1541 → 821	720.11 ± 0.09	720.32 ± 0.03	
730.580 ± 0.028	4.42 ± 0.25	995 → 264	730.72 ± 0.07	730.61 ± 0.03	730.3 ± 0.6
741.298 ± 0.028	107 ± 3	821 → 80	741.43 ± 0.07	741.32 ± 0.03	741.32 <sup>e</sup>
748.290 ± 0.037	0.378 ± 0.024	1569 → 821	748.30 ± 0.10	748.31 ± 0.07	
					773.3 ± 0.5
815.903 ± 0.029	53.5 ± 2.0	896 → 80	816.08 ± 0.07	815.95 ± 0.03	815.95 <sup>e</sup>
821.093 ± 0.029	100 ± 3	821 → 0	821.18 ± 0.08	821.11 ± 0.03	821.11 <sup>e</sup>
829.887 ± 0.035	0.60 ± 0.05	1094 → 264	830.06 ± 0.12	829.91 ± 0.03	
843.764 ± 0.034	0.551 ± 0.020	( <sup>27</sup> Mg)			
853.49 ± 0.06	0.185 ± 0.018	1118 → 264	853.54 ± 0.08	853.47 ± 0.20	
904.95 ± 0.18	0.045 ± 0.008				
914.861 ± 0.031	2.52 ± 0.15	995 → 80	915.01 ± 0.07	914.90 ± 0.03	914.7 ± 0.7
928.84 ± 0.11	0.105 ± 0.014	1193 → 264	929.03 ± 0.12	928.93 ± 0.09	
952.49 ± 0.06	0.158 ± 0.012	1848 → 896	952.45 ± 0.28		
994.93 ± 0.11	0.085 ± 0.008				
1012.05 ± 0.15	0.094 ± 0.012		1012.47 ± 0.15		
1014.10 ± 0.04	0.483 ± 0.019	( <sup>27</sup> Mg)		1014.18 ± 0.05	
1026.96 ± 0.17	0.067 ± 0.013	1848 → 821			
1034.48 ± 0.16	0.064 ± 0.011	1930 → 896			

TABLE V (Continued)

Present work		Assignment From-To	$(n, \gamma)^b$	$^{168}\text{Tm}^c$	$^{168}\text{Ho}^d$
$E_\gamma$ (keV)	$I_{\text{rel}}$		$E_\gamma$ (keV)	$E_\gamma$ (keV)	$E_\gamma$ (keV)
1076.66 ± 0.10	0.090 ± 0.007		1075.2 ± 0.9 1077.6 ± 0.9		
1097.37 ± 0.05	0.254 ± 0.012	( $^{116m}\text{In}$ )			
1104.55 ± 0.22	0.055 ± 0.009		1105.0 ± 0.5		
1108.94 ± 0.30	0.043 ± 0.011	1930 → 821			
1137.21 ± 0.34	0.066 ± 0.022	(2255 → 1118)	1137.2 ± 0.6		
1139.0 ± 0.5	0.040 ± 0.018		1144.02 ± 0.35		
1144.16 ± 0.14	0.075 ± 0.009		1167.37 ± 0.12	1167.49 ± 0.07	
1173.49 ± 0.37	0.40 ± 0.05	$^{60}\text{Co}$ 1995 → 821	1173.87 ± 0.18		
1176.46 ± 0.16	0.078 ± 0.009				
1197.07 ± 0.34	0.036 ± 0.009		1196.55 ± 0.18		
1260.15 ± 0.06	0.265 ± 0.020	2255 → 995			
1264.0 ± 0.4	0.031 ± 0.008		1263.5 ± 0.7		
1267.94 ± 0.11	0.156 ± 0.012				
1273.59 ± 0.04	0.57 ± 0.05				
1277.33 ± 0.06	0.290 ± 0.018	1541 → 264	1277.77 ± 0.25	1277.41 ± 0.04	
1293.73 ± 0.05	0.356 ± 0.015	( $^{116m}\text{In}$ )			
1297.273 ± 0.037	1.00 ± 0.05	2193 → 896	1298.04 ± 0.38		
1341.56 ± 0.26	0.059 ± 0.010				
1350.92 ± 0.35	0.027 ± 0.020	sum peak (1615 → 264)		1351.59 ± 0.05	
1358.99 ± 0.04	0.564 ± 0.025	2255 → 897	1358.80 ± 0.25		
1371.847 ± 0.034	3.8 ± 1.0	2193 → 821	1371.8 ± 0.5		1373 ± 1
1433.67 ± 0.07	0.19 ± 0.05	2255 → 821	1433.5 ± 0.6		
1461.20 ± 0.08	0.243 ± 0.011	1541 → 80		1461.74 ± 0.04	
1488.47 ± 0.44	0.029 ± 0.009			1488.8 ± 0.3	
1507.64 ± 0.20	0.053 ± 0.007	( $^{116m}\text{In}$ )			
1529.12 ± 0.13	0.115 ± 0.012	2425 → 896			1517 ± 1
1541.38 ± 0.23	0.025 ± 0.020	sum peak			
1603.72 ± 0.08	0.337 ± 0.020	2425 → 821			
1651.37 ± 0.21	0.047 ± 0.007		1650.23 ± 0.28		
1711.86 ± 0.21	0.043 ± 0.006				1678 ± 1
1731.19 ± 0.18	0.052 ± 0.006	( $^{24}\text{Na}$ )			
1768.36 ± 0.09	0.75 ± 0.03	1848 → 80			1769 ± 1
1835.45 ± 0.45	0.321 ± 0.013	1915 → 80	1834.70 ± 0.18		
1848.24 ± 0.09	0.71 ± 0.04	1848 → 0			
1850.42 ± 0.10	0.51 ± 0.03	1930 → 80	1850.7 ± 0.8		1850 ± 1
1914.73 ± 0.13	0.133 ± 0.009	1995 → 80	1915.0 ± 0.7		
1930.25 ± 0.10	0.358 ± 0.015	1930 → 0			
2094.83 ± 0.29	0.044 ± 0.007				
2112.46 ± 0.13	0.176 ± 0.010	$^{56}\text{Mn}$ in part			
2127.27 ± 0.19	0.069 ± 0.007	( $^{34m}\text{Cl}$ )			
2175.00 ± 0.27	0.012 ± 0.012	sum peak			
2192.42 ± 0.14	0.010 ± 0.010	sum peak			
2220.72 ± 0.35	0.090 ± 0.021	2485 → 264			
2345.08 ± 0.12	0.602 ± 0.020	2425 → 80			
2379.8 ± 0.6	0.014 ± 0.005				
2390.18 ± 0.37	0.028 ± 0.005				
2404.70 ± 0.16	0.121 ± 0.007	2485 → 80			

TABLE V (Continued)

Present work		Assignment From-To	$(n, \gamma)^b$	$^{168}\text{Tm}^c$	$^{168}\text{Ho}^d$
$E_\gamma$ (keV)	$I_{\text{rel}}$		$E_\gamma$ (keV)	$E_\gamma$ (keV)	$E_\gamma$ (keV)
2424.92 ± 0.14	0.264 ± 0.012	2425 → 0			
2591.57 ± 0.34	0.040 ± 0.007				
2614.40 ± 0.26	0.057 ± 0.007	( $^{208}\text{Tl}$ )			
3102.3 ± 0.5	0.235 ± 0.011	( $^{37}\text{S}$ )			

<sup>a</sup> For comparison purposes, all  $\gamma$  rays observed in  $^{168}\text{Tm}$ -decay studies have been included as well as those neutron-capture  $\gamma$  rays that correspond to  $\gamma$  rays from  $^{168}\text{Ho}$  decay.

<sup>b</sup> See References 10 and 11.

<sup>c</sup> See Reference 8.

<sup>d</sup> See Reference 18.

<sup>e</sup> These  $\gamma$ -ray energies were taken from Ref. 8 and used as calibration lines.

in  $^{168}\text{Ho}$  decay, neutron-capture studies, and  $^{168}\text{Tm}$  decay; intensities are normalized to the 198.221-keV line in  $^{168}\text{Ho}$ . Some weak lines observed in other studies do not appear in  $^{168}\text{Ho}$  spectra due to the Compton background and interfering  $\gamma$  rays from other activities.  $\gamma$  rays at 98.99 and 99.24 keV are unresolved in the present study and in  $^{168}\text{Tm}$  decay, but were resolved in the  $(n, \gamma)$  work<sup>10</sup> with a bent-crystal spectrometer. Values shown in parentheses were computed using the 98.99- to 928.84-keV and 99.24- to 198.221-keV intensity ratios determined from the  $(n, \gamma)$  results and adjusted to give the total 99-keV intensity measured in this study. Table VII indicates some inconsistency in intensity values of the 99.24- and 829.887-keV lines as measured in different studies.

The half-life of the 1093.898-keV level (115.7 ± 3.3 ns),<sup>5</sup> decay mode (strong deexcitation to the 3<sup>+</sup>2 and 4<sup>+</sup>2 levels), and transition multipolarities support the previously assigned  $I^\pi K$  values of 4<sup>-</sup>4. The 1192.89-keV level has been identified as the 5<sup>-</sup>4 member of the 1093.898-keV band. In  $^{168}\text{Ho}$  it is observed to decay strongly to the band head and weakly (due to a  $K$  forbiddenness of 3) to the 4<sup>+</sup>0 level at 264.067 keV.

Harlan and Sheline<sup>13</sup> measured a large cross section for population of the 1093.898-keV band in the  $(d, p)$  reaction on  $^{167}\text{Er}$ . This gives strong support for the two-quasineutron assignment [633<sup>+</sup> + 521<sup>+</sup>].  $\beta$  decay from  $^{168}\text{Ho}$  to the 4<sup>-</sup>4 band head should proceed as a first-forbidden decay, but with an additional large forbiddenness factor due to a  $\Delta\Omega$  of 7. The low measured  $\log ft$  (7.3) is therefore difficult to understand. However, the  $\log ft$  is poorly determined due to effects of  $\gamma$ -ray summing in the detector. In  $^{168}\text{Ho}$  decay,  $\gamma$  intensity into the 5<sup>-</sup>4 level appears to exceed the intensity of deexcitation  $\gamma$  rays. This is probably the result of an unresolved  $\gamma$  peak at 198.24 keV (see Table VIII) of intensity  $\geq 0.36$ . A lower limit

of 8.0 can be placed on the  $\log ft$  for decay to the 5<sup>-</sup>4 level.

#### D. $K^\pi = 3^-$ Band at 1541.33 keV

The first five levels of the 1541.33-keV band have been identified in  $(n, \gamma)^{10,11}$  and  $(d, p)^{13}$  studies, and the first two were observed in  $^{168}\text{Tm}$

TABLE VI. Levels of  $^{168}\text{Er}$  populated by the  $\beta$  decay of  $^{168}\text{Ho}$ .

Level (keV)	$I^\pi K$	$E_\beta$ (MeV)	% of total decays	$\log ft^a$
0	0 <sup>+</sup> 0	3.00		
79.800 ± 0.001 <sup>b</sup>	2 <sup>+</sup> 0	2.92		
264.067 ± 0.014	4 <sup>+</sup> 0	2.74		
(548.45 ± 0.07)	6 <sup>+</sup> 0	2.45	≤ 0.046	≥ 8.9
821.109 ± 0.023	2 <sup>+</sup> 2	2.18	71.0	5.6
895.711 ± 0.025	3 <sup>+</sup> 2	2.10	19.4	6.2
994.654 ± 0.028	4 <sup>+</sup> 2	2.01	1.94	7.1
1093.898 ± 0.031	4 <sup>-</sup> 4	1.91	~ 0.8	≥ 7.3
1117.56 ± 0.06	5 <sup>+</sup> 2	1.88	≤ 0.042	≥ 8.7
1192.89 ± 0.10	5 <sup>-</sup> 4	1.81	Small	
1541.33 ± 0.04	3 <sup>-</sup> 3	1.46	2.54	6.6
(1569.40 ± 0.05)	2 <sup>-</sup> 2	1.43	0.134	7.8
1615.17 ± 0.11	4 <sup>-</sup> 3	1.38	0.24	7.5
1848.20 ± 0.06	(2 <sup>+</sup> 2)	1.15	0.59	6.8
1915.29 ± 0.09	(3 <sup>+</sup> 2)	1.08	≤ 0.131	≥ 7.4
1930.23 ± 0.07	(2 <sup>+</sup> 2)	1.07	≤ 0.346	≥ 7.0
(1994.60 ± 0.06)	(3 <sup>+</sup> 2)	1.01	≤ 0.191	≥ 7.1
2192.97 ± 0.05	(2 <sup>-</sup> 2)	0.81	1.7	5.9
2254.75 ± 0.07	(3 <sup>-</sup> 2)	0.75	≤ 0.38	≥ 6.4
2424.87 ± 0.07	(2 <sup>+</sup> 2)	0.58	≤ 0.466	≥ 5.9
2484.57 ± 0.14	(3 <sup>+</sup> 2)	0.52	≤ 0.074	≥ 6.6

<sup>a</sup>  $\log ft$  values were determined using the Moszkowski nomogram [S. A. Moszkowski, Phys. Rev. **82**, 35 (1951)]. Errors are ± 0.1. However, this does not include a contribution due to errors in the value of  $E_\beta$ , which may be large for high-energy levels.

<sup>b</sup> Determined by Koch (Ref. 10).

TABLE VII. Relative transition probabilities from the  $K^\pi = 2^+$  band at 821.109 keV.

Level	$E_\gamma$	$E_{\text{final}}$	$I^\pi K$	$B(E2)_{\text{rel}}$	$B(E2)_{\text{theory}}^a$	
					$z_2 = 0$	$36.7 \times 10^{-3}$
821.109	557.012	264.067	$4^+0$	$0.075 \pm 0.004$	0.050	0.077
	741.298	79.800	$2^+0$	1.000	1.000	1.000
	821.093	0	$0^+0$	$0.560 \pm 0.011$	0.700	0.564
895.711	631.670	264.067	$4^+0$	$0.64 \pm 0.04$	0.40	0.64
	815.903	79.800	$2^+0$	1.00	1.00	1.00
994.654	730.580	264.067	$4^+0$	1.00	1.00	1.00
	914.861	79.800	$2^+0$	$0.19 \pm 0.02$	0.34	0.20
1117.56	853.487	264.067	$4^+0$			

<sup>a</sup> For a description of the theory in the strong-coupling limit and with band mixing, see O. Nathan and S. G. Nilsson, in *Alpha-, Beta-, and Gamma-ray Spectroscopy*, edited by K. Siegbahn (North-Holland, Amsterdam, 1965), Vol. 1, p. 601.

decay.<sup>8</sup> We have also seen the first two levels of the band in  $^{168}\text{Ho}$  decay. Table IX shows the  $\gamma$  rays that deexcite the 3-3 level at 1541.33 keV and the 4-3 level at 1615.17 keV as measured in decay and  $(n, \gamma)$  studies. Intensities are normalized to that of the 447.461-keV line. Results of  $^{168}\text{Ho}$  and  $^{168}\text{Tm}$  decay are generally in agreement. Several weak lines observed in the  $(n, \gamma)$  spectrum could not be seen in decay studies. Michaelis, Ottmar, and Weller<sup>11</sup> have attributed the large discrepancies of the  $(n, \gamma)$  intensities to the population of a  $4^-1$  level very close to the 1541.33-keV level.

Harlan and Sheline<sup>13</sup> have assigned to the 1541.33-keV band the two-quasineutron configuration  $[633\uparrow - 521\uparrow]$ . This is consistent with  $\beta$ -de-

cay results, as both  $^{168}\text{Ho}$  and  $^{168}\text{Tm}$  can populate the  $[633\uparrow - 521\uparrow]$  configuration by a one-quasiparticle change.  $\text{Log}ft$  values in  $^{168}\text{Ho}$  decay are 6.6 to the 3-3 level and 7.5 to the 4-3 level. Both are in the range expected for first-forbidden decays. The corresponding values in  $^{168}\text{Tm}$  decay<sup>8</sup> are 7.1 and 8.9.

Reduced  $\gamma$ -transition ratios for this band are computed and tabulated by Gunther and Parsignault.<sup>5</sup> The present results are in qualitative agreement with those of Ref. 5, which were found to be most consistent with a  $K$  value of 3. However, agreement with theory was found not to be sufficient for a  $K$  assignment to be made from  $\gamma$ -transition intensities alone and indicates a significant amount of configuration mixing.

TABLE VIII.  $\gamma$  intensities from levels of the  $K^\pi = 4^-$  band at 1093.898 keV.

Level	$E_\gamma$ (keV)	$E_{\text{final}}$ (keV)	$I^\pi K$	Intensity <sup>a</sup>		
				$^{168}\text{Ho}$	$^{168}\text{Tm}$ <sup>b</sup>	$(n, \gamma)$ <sup>c</sup>
1093.898	99.24	994.654	$4^+2$	(0.58)	(0.60)	0.43
	198.221	895.711	$3^+2$	7.1	7.1	7.1
	272.79	821.109	$2^+2$		0.014	0.015
	829.887	264.067	$4^+0$	0.60	0.88	1.03
1192.89	75.33	1117.56	$5^+2$			0.0016
	98.99	1093.898	$4^-4$	(0.27)	(0.023)	0.58
	198.24	994.654	$4^+2$	Unresolved from the 198.221-keV $\gamma$ ray		
	297.18	895.711	$3^+2$			0.0021
928.84	264.067	$4^+0$	0.11	0.0078	0.32	

<sup>a</sup> Values in parentheses were obtained from measured values and  $(n, \gamma)$   $\gamma$ -intensity ratios. See text for elaboration.

<sup>b</sup> See Reference 8.

<sup>c</sup> See Reference 10.

TABLE IX. Transition intensities from levels of the  $K^\pi = 3^-$  band at 1541.33 keV.

$E_{\text{level}}$	$E_\gamma$ (keV)	$E_{\text{level}}$ (keV)	$I^\pi K$	Intensity <sup>a</sup>		
				$^{168}\text{Ho}$	$^{168}\text{Tm}$ <sup>b</sup>	$(n, \gamma)$ <sup>c</sup>
1541.33	348.51	1192.89	$5^-4$		0.056	0.079
	447.461	1093.898	$4^-4$	4.0	4.0	4.0
	546.73	994.654	$4^+2$	0.46	0.43	1.5
	645.56	895.711	$3^+2$	0.31	0.26	1.2
	720.171	821.109	$2^+2$	2.2	2.0	3.8
	1277.33	264.067	$4^+0$	0.29	0.29	4.0
1461.20	79.800		$2^+0$	0.24	0.060	
1615.17	(211.41)	1403.87	$2^-1$			0.0043
	303.82	1311.50	$6^-4$			0.024
	422.278	1192.89	$5^-4$	0.65	0.049	2.1
	497.83	1117.56	$5^+2$			0.46
	521.39	1093.898	$4^-4$			0.28
	1350.92	264.067	$4^+0$		$\leq 0.027$	

<sup>a</sup> Intensities are normalized to the 447.461-keV transition in each case.

<sup>b</sup> See Reference 8.

<sup>c</sup> See Reference 10.

## E. Level at 1569.40 keV

Michaelis, Ottmar, and Weller<sup>11</sup> identified a band at 1569.48 keV from thermal-neutron-capture spectra. The  $2^-$  to  $5^-$  levels were observed at 1569.48, 1633.63, 1719.22, and 1827.57 keV. Based on their work and results of resonance-capture,<sup>12</sup> ( $d, p$ ),<sup>13</sup> and ( $d, d'$ )<sup>14</sup> studies, they identified this band as the  $K^\pi = 2^-$  octupole vibration. Both of the lowest-lying two-quasiparticle configurations that might contribute to the band ( $[642\uparrow - 521\uparrow]_{mn}$  and  $[411\uparrow - 523\uparrow]_{pp}$ ) can be populated from <sup>168</sup>Ho by a change of one quasiparticle.

No  $\gamma$  transitions from levels of the 1569.48-keV band to the ground-state band were observed by Michaelis *et al.* The most intense transitions were to low-lying levels of the  $\gamma$  band. Of these, transitions from the  $3^-$  and  $4^-$  levels lie under peaks from  $\gamma$ -band deexcitation in the 700- to 900-keV region, which are very intense in <sup>168</sup>Ho-decay spectra. However, we have observed a 748.290-keV  $\gamma$  ray, which corresponds closely to the 748.30-keV transition from the 1569.46-keV level to the  $2^+2$  member of the  $\gamma$  band. Weaker transitions from this level do not rise above background in the <sup>168</sup>Ho spectrum.

The  $\log ft$  value for decay to the 1569.40-keV level is 7.8. The corresponding value in <sup>169</sup>Tm decay<sup>5</sup> is 8.9. The higher  $\log ft$  in the decay of <sup>168</sup>Tm to this band may result from the fact that a transition to the  $[411\uparrow - 523\uparrow]_{pp}$  configuration cannot occur without a two-quasiparticle change.

## F. Band at 1848.20 keV

Evidence for a level at 1848.20 keV is provided by  $\gamma$  rays having energies consistent with transitions to the  $0^+$  and  $2^+$  levels of the ground-state band, and  $2^+$  and  $3^+$  levels of the  $\gamma$  band. Transitions to the  $3^+$  and  $4^+$  levels of the  $\gamma$  band would, if present, be obscured by other intense  $\gamma$  rays. Possible spin and parity values are  $1^+$  and  $2^+$ . A  $\log ft$  of 6.8 favors the  $2^+$  (allowed) over the  $1^+$  (second-forbidden) assignment. The  $2^+$  assignment is further supported by the presence of a level in resonance capture<sup>12</sup> at  $1848.3 \pm 0.4$  keV having a spin and parity of  $2^+$  or  $5^+$ .

We also find evidence for a level at 1915.29 keV with  $\gamma$  transitions to the  $2^+$  and  $4^+$  members of the ground-state band. Spin and parity values for this level are limited to  $2^+$ ,  $3^+$ , and  $4^+$ . A level at 1914.36 keV having a spin and parity of  $3^-$  or  $4^-$  was observed in ( $n, \gamma$ ).<sup>11</sup> Although it is close to the 1915.29-keV level, the energy difference ( $0.93 \pm 0.17$  keV) indicates that the two are different levels. Two levels near 1914 keV were also observed in other studies, but with energy errors large enough for them to be associated

TABLE X. Relative transition probabilities from the  $K^\pi = 2^+$  band at 1848.20 keV.

Level	$E_\gamma$ (keV)	$E_{\text{final}}$ (keV)	$I^\pi K$	$B(E2)_{\text{exp}}$	$B(E2)_{\text{theory}}$	
					$K=2$	$K=1$
1848.20	952.49	895.711	$3^+2$	$0.21 \pm 0.02$		
	1026.96	821.109	$2^+2$	$0.09 \pm 0.02$		
		264.067	$4^+0$		0.05	3.20
	1768.36	79.800	$2^+0$	1.00	1.00	1.00
1848.25		0	$0^+0$	$0.75 \pm 0.05$	0.70	2.80
	1915.29	1651.37	$4^+0$	$0.25 \pm 0.04$	0.40	2.50
	1835.45	79.800	$2^+0$	1.00	1.00	1.00

with either the 1914.36- or the 1915.29-keV level. Each is consistent with a spin and parity of  $3^-$  [ $1914.0$  keV ( $3^-$  or  $4^-$ ) in resonance capture<sup>12</sup> and  $1910$  keV ( $3^-$  or  $4^+$ ) in ( $d, d'$ )<sup>14</sup>].

We propose that the levels at 1848.20 and 1915.29 keV are the  $2^+$  and  $3^+$  members of a  $K=2$  band for the following reasons:

- (1) The ratio [ $\log ft(3^+)/\log ft(2^+)$ ] of 7.4/6.8 compares well with theory<sup>28</sup> which gives a ratio of 7.3/6.8;
- (2) branching ratios of  $\gamma$  transitions to the ground-state band, assuming  $E2$  multiplicities (see Table X), are in reasonable agreement with theoretical values; and
- (3) a moment of inertia  $\mathcal{I} = 1.20 \mathcal{I}_{\text{g.s.}}$  is in qualitative agreement with the moments of inertia of excited bands ( $\mathcal{I}_{\gamma \text{ band}} = 1.07 \mathcal{I}_{\text{g.s.}}$  and  $\mathcal{I}_{\beta \text{ band}} = 1.34 \mathcal{I}_{\text{g.s.}}$ ) generally observed in rotational nuclei.

A level at 1843 keV was populated in inelastic deuteron scattering,<sup>14</sup> which gives evidence that the 1848.20-keV band has a collective character.

## G. Levels at 1930.23 and 1994.60 keV

The presence of a level at 1930.23 keV is indicated by transitions to the  $0^+$  and  $2^+$  levels of the ground-state band, as well as to the  $2^+$  and  $3^+$  levels of the  $\gamma$  band. The most intense transition, at 1850.42 keV, may have been observed in thermal-neutron capture,<sup>11</sup> but was not assigned. Spin and parity possibilities are  $1^+$  and  $2^+$ , with the  $\log ft$

TABLE XI. Relative transition probabilities from the  $K^\pi = 2^-$  band at 2192.97 keV.

Level	$E_\gamma$ (keV)	$E_{\text{final}}$ (keV)	$I^\pi K$	$B(E1)_{\text{exp}}$	$B(E1)_{\text{theory}}$	
					$K=2$	$K=1$
2192.97	1297.273	895.711	$3^+2$	$0.32 \pm 0.08$	0.50	2.00
	1371.847	821.109	$2^+2$	1.00	1.00	1.00
2254.75	1137.21	1117.56	$5^+2$	$(0.07 \pm 0.02)$		
	1260.15	994.654	$4^+2$	$0.56 \pm 0.05$	1.29	1.29
	1358.99	895.711	$3^+2$	1.00	1.00	1.00
	1433.67	821.109	$2^+2$	$0.28 \pm 0.02$	0.71	0.11

TABLE XII. Relative transition probabilities from the  $K^\pi = 2^+$  band at 2424.87 keV.

Level	$E_\gamma$ (keV)	$E_{\text{final}}$ (keV)	$I^\pi K$	$B(E2)_{\text{exp}}$	$B(E2)_{\text{theory}}$	
					$K=2$	$K=1$
2424.87	1529.12	895.711	$3^+2$	$0.19 \pm 0.02$		
	1603.72	821.109	$2^+2$	$0.56 \pm 0.04$		
	2345.08	79.800	$2^+0$	1.00	1.00	1.00
	2424.92	0	$0^+0$	$0.37 \pm 0.02$	0.70	2.80
2484.57	2220.72	264.067	$4^+0$	$1.1 \pm 0.3$	0.4	2.5
	2404.70	79.800	$2^+0$	1.0	1.0	1.0

of 7.0 favoring the latter. A level at  $1930.8 \pm 0.8$  keV was observed in resonance capture<sup>12</sup> and was also assigned a positive parity. The  $\gamma$ -branching intensities suggest a  $K$  value of 2. The reduced intensity ratio, assuming  $E2$  multipolarities, of transitions to the  $0^+$  and  $2^+$  levels of the ground-state band is 0.56, compared to theoretical values of 0.70 ( $K=2$ ) and 2.80 ( $K=1$ ).

A level at 1994.60 keV is suggested by the energy fit of  $\gamma$  rays to the  $2^+$  levels of the ground-state and  $\gamma$  bands. Most probable spin and parity values in the absence of a transition to the ground state are  $2^-$ ,  $3^+$ , or  $4^+$ . The energy separation of the 1930.23- and the proposed 1994.60-keV levels and the corresponding moment of inertia  $\mathcal{J} = 1.24 \mathcal{J}_{\text{g.s.}}$  suggest that they form the  $2^+$  and  $3^+$  members of a  $K=2$  band. The above interpretation should be viewed with caution, however, because of the presence of a level at  $1995.6 \pm 2.0$  keV in resonance capture, with a spin and parity of  $2^-$  or  $5^-$ .

#### H. Band at 2192.97 keV

Level placements at 2192.97 and 2254.75 keV are based on the observation of  $\gamma$  rays populating levels of the  $\gamma$  band and on the detection of weak sum peaks. The 2192.97-keV level is deexcited by  $\gamma$  transitions to the  $2^+$  and  $3^+$  levels of the  $\gamma$  band. A peak in the  $\gamma$  spectrum at 2192.42 keV can be attributed to summing of a cascade through the  $2^+$  level of the  $\gamma$  band. Most probable spin and parity values in the absence of a transition to the ground state are  $2^-$ ,  $3^+$ , and  $4^+$ .

The 2254.75-keV level populates the  $2^+$ ,  $3^+$ ,  $4^+$ , and possibly the  $5^+$  levels of the  $\gamma$  band. However, the 1137.21-keV  $\gamma$  ray may deexcite the  $0^+$  level of the  $\beta$  band,<sup>11</sup> rather than populating the  $5^+$  level of the  $\gamma$  band as interpreted above. A sum peak is observed due to cascades through the  $3^+$  and  $4^+$  levels of the  $\gamma$  band. The  $\log ft$  for population of the 2254.75-keV level is 6.4. Spin and parity values are limited to  $3^+$  and  $4^+$ .

Two weak  $\gamma$  rays were observed in thermal-neu-

tron capture<sup>11</sup> with energies corresponding to the most intense transitions from both the 2192.97- and 2254.75-keV levels; neither was placed in the previous level scheme. A weak peak was observed in  $(d, p)^{13}$  excitation corresponding to a level at 2255 keV, which may be the 2254.75-keV level. Most significant, however, is the presence of an intense peak in inelastic deuteron scattering<sup>14</sup> indicating a collective level at 2257 keV having a spin and parity of  $3^-$ . This energy value is within error of the 2254.75-keV level. It is proposed, therefore, that the 2192.97- and 2254.75-keV levels are the  $2^-$  and  $3^-$  members of a  $K=2$  band for the following reasons:

- (1) Both levels are strongly populated by  $\beta$  decay ( $\log ft$  values of 5.9 and 6.4, respectively) while no other levels within 150 keV are populated with sufficient intensity to be identified;
- (2) both deexcite (see Table XI) only to the  $\gamma$  band (transitions from a  $K^\pi = 2^-$  band to the ground-state band should be weak); and,
- (3) the energy separation gives a moment of inertia  $\mathcal{J} = 1.29 \mathcal{J}_{\text{g.s.}}$ .

#### I. Levels at 2424.87 and 2484.57 keV

The presence of a level at 2424.87 keV is indicated by the energies of  $\gamma$  transitions to the  $0^+$  and  $2^+$  levels of the ground-state band, and the  $2^+$  and  $3^+$  levels of the  $\gamma$  band. Possible spin and parity values are  $1^+$  and  $2^+$ . The  $\log ft$  of 5.9 favors the  $2^+$  assignment. Placement of the 2484.57-keV level is based on  $\gamma$  rays populating the  $2^+$  and  $4^+$  levels of the ground-state band. Most probable spin and parity values in the absence of a transition to the ground state are  $3^+$  and  $4^+$ . It is suggested that these levels are the  $2^+$  and  $3^+$  members of a  $K=2$  band because:

- (1) The energy separation gives a moment of inertia  $\mathcal{J} = 1.35 \mathcal{J}_{\text{g.s.}}$ ; and,
- (2)  $\gamma$ -transition intensities (see Table XII) weakly favor a  $K$  of 2.

A level populated by  $(d, p)^{13}$  was observed at 2430 keV and another may have been observed at 2478 keV. These may be the 2424.87- and 2484.57-keV levels and, if so, would suggest a two-quasi-neutron configuration.

#### V. SUMMARY

Several rotational bands in  $^{168}\text{Er}$  seen in other studies have been observed in the  $\beta$  decay of  $^{168}\text{Ho}$ . These include the ground-state,  $\gamma$  and  $K^\pi = 2^-$  octupole bands, and the  $K^\pi = 4^-$  and  $3^-$  bands at 1093.898 and 1541.33 keV, respectively. Our results are consistent with the interpretations

that have been presented previously for these bands. The  $\beta$  decay to these bands, including the strong decay to the  $\gamma$  band, supports a  $3^+3$  assignment for the  $^{168}\text{Ho}$  ground state with a  $pn$  configuration  $[523^+ - 521^\dagger]$  predominating.

Several additional  $^{168}\text{Er}$  bands have been tentatively identified. Evidence from inelastic deuteron scattering<sup>13</sup> indicates that  $K^\pi = 2^+$  and  $2^-$  bands at 1848.20 and 2192.97 keV, respectively, are predominantly collective. Bands at 1930.23 and 2424.87 keV have  $K^\pi = 2^+$  as the most probable  $K$  value. Evidence from the  $(d, p)$ <sup>12</sup> reaction fa-

vors a two-quasineutron configuration for the 2424.87-keV band.

#### ACKNOWLEDGMENTS

We wish to thank E. M. Lent for considerable work in developing the computer programs used for data analysis. We are indebted to D. H. White and R. E. Birkett for making their peak-fitting routines available. We wish to thank T. Valk for continued assistance with the electronic and detector systems.

<sup>†</sup>Work performed under the auspices of the U. S. Atomic Energy Commission.

<sup>1</sup>K. P. Jacob, J. W. Mihelich, B. Harmatz, and T. H. Handley, *Phys. Rev.* **117**, 1102 (1960).

<sup>2</sup>J. J. Reidy, E. G. Funk, and J. W. Mihelich, *Phys. Rev.* **133**, B556 (1964).

<sup>3</sup>J. Jursík and V. Zvolská, *Nucl. Phys.* **86**, 405 (1966).

<sup>4</sup>V. A. Bondarenko and P. T. Prokof'ev, *Izv. Akad. Nauk SSSR Ser. Fiz.* **30**, 1173 (1966) [transl.: *Bull. Acad. Sci. USSR, Phys. Ser.* **30**, 1225 (1966)].

<sup>5</sup>C. Gunther and D. R. Parsignault, *Phys. Rev.* **153**, 1297 (1967).

<sup>6</sup>Z. N. Mimoshevili and A. A. Sorokin, *Izv. Akad. Nauk SSSR Ser. Fiz.* **32**, 139 (1968) [transl.: *Bull. Acad. Sci. USSR, Phys. Ser.* **32**, 133 (1968)].

<sup>7</sup>P. F. Kenealy, E. G. Funk, and J. W. Mihelich, *Nucl. Phys.* **A110**, 561 (1968).

<sup>8</sup>G. E. Keller, E. F. Zganjar, and J. J. Pinajian, *Nucl. Phys.* **A129**, 481 (1969).

<sup>9</sup>L. V. Groshev, A. M. Demidov, V. A. Ivanov, V. N. Lutsenko, V. I. Pelekhov, and N. Shadiev, *Izv. Acad. Nauk SSSR Ser. Fiz.* **29**, 772 (1965) [transl.: *Bull. Acad. Sci. USSR, Phys. Ser.* **29**, 775 (1965)].

<sup>10</sup>H. R. Koch, *Z. Physik* **192**, 142 (1966).

<sup>11</sup>W. Michaelis, H. Ottmar, and F. Weller, *Nucl. Phys.* **A150**, 161 (1970).

<sup>12</sup>L. M. Bollinger and G. E. Thomas, *Phys. Rev. C* **2**, 1951 (1970).

<sup>13</sup>R. A. Harlan and R. K. Sheline, *Phys. Rev.* **160**, 1005 (1967).

<sup>14</sup>P. O. Tjøm and B. Elbek, *Nucl. Phys.* **A107**, 385 (1968).

<sup>15</sup>Y. Yoshizawa, B. Elbek, B. Herskind, and M. C. Olesen, *Nucl. Phys.* **73**, 273 (1965).

<sup>16</sup>R. G. Wille and R. W. Fink, *Phys. Rev.* **118**, 242 (1960).

<sup>17</sup>K. Takahashi, T. Kuroyanagi, H. Yuta, K. Kotajima, K. Nagatani, and H. Moringa, *J. Phys. Soc. Japan* **16**, 1664 (1961).

<sup>18</sup>P. E. Haustein and A. B. Tucker, *Nucl. Phys.* **A173**, 321 (1971).

<sup>19</sup>R. Booth and H. H. Barschall, *Nucl. Instr. Methods* **99**, 1 (1972).

<sup>20</sup>E. A. Nawrocki, K. G. Tirsell, and L. G. Multhauf, to be published.

<sup>21</sup>D. C. Camp and G. L. Meredith, *Nucl. Phys.* **A166**, 349 (1971).

<sup>22</sup>R. J. Gehrke, J. E. Cline, and R. L. Heath, *Nucl. Instr. Methods* **91**, 349 (1971).

<sup>23</sup>G. F. Meredith and R. A. Meyer, *Nucl. Phys.* **A142**, 513 (1970).

<sup>24</sup>S. Raman and J. J. Pinajian, *Nucl. Phys.* **A131**, 393 (1969).

<sup>25</sup>R. G. Helmer, R. C. Greenwood, and R. J. Gehrke, *Nucl. Instr. Methods* **96**, 173 (1971).

<sup>26</sup>R. C. Greenwood and W. W. Black, *Phys. Letters* **21**, 702 (1966).

<sup>27</sup>D. R. Bès, P. Federman, E. Maqueda, and A. Zuker, *Nucl. Phys.* **65**, 1 (1965).

<sup>28</sup>C. J. Gallagher, Jr., and V. G. Soloviev, *Kgl. Danske Videnskab. Selskab, Mat.-Fys. Skrifter* **2**, 2 (1962).